Max-Planck-Institut
für Meteorologie

# REPORT No. 108

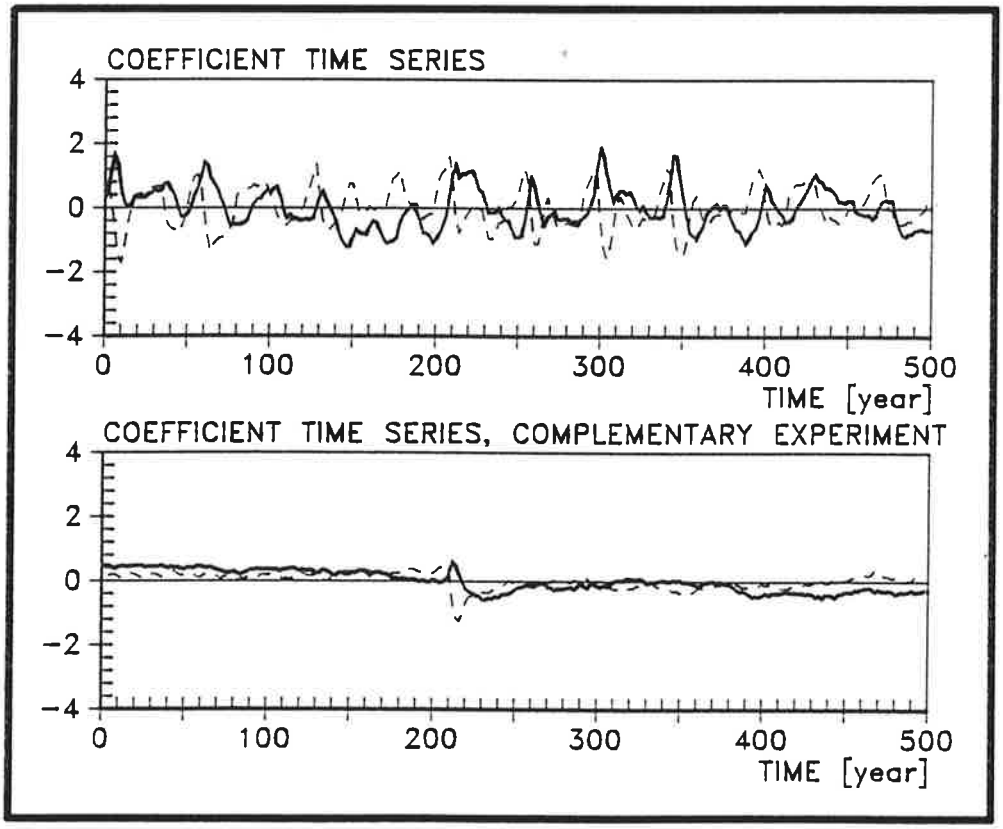


# DECADAL VARIABILITY OF THE NORTH ATLANTIC IN AN OCEAN GENERAL CIRCULATION MODEL

von

RALF WEISSE • UWE MIKOLAJEWICZ • ERNST MAIER-REIMER

HAMBURG, JULY 1993

AUTHORS:

Ralf Weisse
Uwe Mikolajewicz
Ernst Maier-Reimer

Max-Planck-Institut
für Meteorologie

MAX-PLANCK-INSTITUT
FÜR METEOROLOGIE
BUNDESSTRASSE 55
D-20146 Hamburg
F.R. GERMANY

Tel.: +49 (40) 4 11 73-0
Telex: 211092 mpime d
Telemail: MPI.METEOROLOGY
Telefax: +49 (40) 4 11 73-298

REPb108

# Decadal Variability of the North Atlantic

# in an

# Ocean General Circulation Model

Ralf Weisse, Uwe Mikolajewicz and Ernst Maier-Reimer

Max-Planck-Institut für Meteorologie
Bundesstrasse 55, 20146 Hamburg, F.R. Germany

ISSN 0937–1060

# ABSTRACT

Climatic fluctuations on a decadal time-scale in the North Atlantic in a global OGCM were considered. The analysis was carried out for the 3800 year stochastic forcing simulation of Mikolajewicz and Maier-Reimer in which the Hamburg Large-Scale Geostrophic Ocean Model was driven by monthly climatologies of windstress, air temperature and fresh water flux with superimposed temporally white noise fresh water fluxes with an amplitude of about 16mm/month.

We applied a Principal Oscillation Pattern analysis to the vector time series of the upper level salinity fields so that the examined fluctuations appear as estimated eigenmodes of the system. In addition to an oscillation with a period of 320 years as already described by Mikolajewicz and Maier-Reimer, we found a broad band Principal Oscillation Pattern with time-scales in the order of 10 to 40 years. It describes the generation of salinity anomalies in the Labrador Sea and the following discharge into the North Atlantic. In sensitivity experiments we clarified that the source of the variability lies in the Labrador Sea and showed that the generation of the salinity anomalies is mainly due to an undisturbed local integration of the white noise fresh water fluxes.

# 1. INTRODUCTION

In the last few years, the problem of natural climate variability has attracted increasing attention from the scientific community, especially in the context of the detection of the greenhouse signal in observed climate records. Until now, our knowledge about climate variations on decadal or longer time-scales is rather poor. The major difficulty in this time-scale range is the insufficient data base. With few exceptions, instrumental records are generally shorter than 100 years. Corrections for changes in the measurement technique, urbanization effects etc. are often as large as the signal itself. Many available time series of proxy data do have the required length and resolution, but the direct physical interpretation of these data is often difficult due to ambiguous transfer functions, dating problems etc. Comprehensive overviews are given by Folland et al. (1990) and Crowley and North (1991).

More information is available on shorter time-scales. The El Niño/Southern Oscillation phenomenon is probably the best known and most studied example of natural climate variability (e.g. Rasmusson and Carpenter 1982). The characteristic time-scale of this process is only a few years and the observational base for the analysis is relatively good. Another region where shorter time-scale variations have been extensively investigated is the North Atlantic. Most of the oceanic heat transport and deep-water production is located in the Atlantic, and thus, changes in the Atlantic circulation and deep convection may have great impact on climate. An intriguing example is the "Great Salinity Anomaly" (GSA) observed in the 70s in the Northern North Atlantic. Dickson et al. (1988) interpreted it as a negative salinity anomaly being advected around the subpolar gyre. On its path, it reduced convection, increased sea-ice cover near Iceland and lowered surface temperatures. Levitus (1989a,b) showed the 3-dimensional extent of the anomaly in the North Atlantic by comparing data from 1970-74 vs. data from 1955-59. He came up with a picture consistent with the early stages of the GSA.

Bjerknes (1964) investigated air-sea interaction in the North Atlantic region on both interannual and interdecadal time-scales. Using data covering the 1890-1940 period, he formulated the hypothesis that the interannual variability is mainly due to local air-sea interaction, whereas the

interdecadal variations are results of a slow and non-local dynamical interaction. Using more than a century of SST observations, Kushnir (1993) came to similar conclusions. Deser and Blackmon (1993) emphasized the irregularity of the decadal variations and argued that there are no differences in the ocean-atmosphere interaction on the interannual and interdecadal time-scales. Among other possibilities to explain the decadal variability, they demonstrated that the sea-ice concentration in the Labrador Sea leads the "decadal pattern" of SST by roughly 2 years, indicating that the processes in marginal Seas can play a major role in the overall dynamics of the North Atlantic.

Due to the sparsity of data, attempts to understand the principal physics of natural climate variability have often been made using models. Early attempts to study the influence of short-term atmospheric variability on long-term oceanic variability have been based on the concept of stochastic climate models as proposed by Hasselmann (1976). The atmosphere is assumed to adjust to a quasi-equilibrium on time-scales of decades and longer. The low frequency variance spectrum is governed by the internal dynamics of the ocean. The integration of the short-term atmospheric fluctuations transforms the essentially white noise[1] atmospheric forcing into a red response signal. For a linear system the resulting response spectrum is proportional to $\omega^{-2}$ as long as the frequency $\omega$ is large compared to the inverse of the natural time-scales of the slow system, and constant for low frequencies. Simple models consisting typically of one (or more) boxes, a linear feedback term and a forcing term have been successfully applied to the global ocean by Lemke (1977) and Wigley and Raper (1990), and to the surface ocean by Frankignoul and Hasselmann (1977), Frankignoul and Reynolds (1983) and Herterich and Hasselmann (1987).

Recent investigations have considered decadal and century scale variability in circulation models. Mikolajewicz and Maier-Reimer (1990) applied the concept of the stochastic climate models to an ocean general circulation model (OGCM). They forced their OGCM with white noise fresh water fluxes and obtained a

---

[1]The variance spectrum of a white noise process is constant. All frequencies provide the same contribution to the total variance of the process. The circumstances are similar to white light. A red noise process however, is defined by higher energy in the low frequency range.

dominant, irregular oscillation with a period of about 320 years. The mechanism responsible for this effect was the advection of salinity anomalies by the mean thermohaline circulation of the Atlantic. Mikolajewicz and Maier-Reimer (1991) showed that the amplitude of the forcing was a critical parameter for the occurrence of the mode. Mysak et al. (1993) performed similar experiments with a zonally integrated ocean model and investigated the response as a function of parameters such as amplitude of forcing and horizontal and vertical diffusivities. Over a wide range of parameters they, too, obtained dominant modes with periods between 200 and 300 years. Other authors report on selfsustaining oscillations in models with idealized topography with a period of a few decades (e.g. Marotzke 1990, Weaver et al. 1991) or a few centuries (e.g. Winton and Sarachik 1992). Delworth et al. (1993) described an irregular oscillation of the thermohaline circulation in the North Atlantic in a fully coupled ocean-atmosphere GCM. This appeared to be an oscillatory mode of the ocean system alone, driven by density anomalies at the site of formation of North Atlantic deep water, while the atmospheric feedback seemed to be small.

In the present study, we analyzed surface and sub-surface data from the stochastically forced OGCM experiment of Mikolajewicz and Maier-Reimer with special attention to the North Atlantic region, motivated by the observational evidence for the existence of decadal variability in nature. The experiment, performed with an OGCM including a realistic bathymetry, yielded sufficiently long time-series to investigate decadal variability. We found a dominant mode on a decadal time-scale in the North Atlantic region.

In Section 2, we briefly describe the model and the stochastically forced experiment. A brief outline of the Principal Oscillation Pattern technique is given in Section 3. In Chapter 4, we describe the dominant decadal mode in the Northern North Atlantic and suggest a hypothetical mechanism. Some sensitivity experiments in support of this explanation are presented in Section 5 together with an intercomparison to the results of the basic experiment. In Section 6, our results are summarized and discussed.

# 2. Model and Experiment

## 2.1 The Model and Spinup

The Hamburg Large-Scale-Geostrophic OGCM, whose concept was originally proposed by Hasselmann (1982), is especially designed for the study of slow climatic variations. An implicit integration method permits a time step of 30 days, thus, allowing integrations over thousands of years at acceptable computing costs. Basic features of this model are described in Maier-Reimer and Hasselmann (1987). Details are presented in Maier-Reimer et al. (1993) in which the sensitivity of the steady state ocean circulation to different formulations of the upper boundary condition for heat and salt is discussed. From a series of experiments with varying boundary conditions a standard run was defined which best reproduces the observed large-scale thermohaline circulation.

The model is based on the conservation laws for heat, salt and momentum (the latter in a linearized form), the full equation of state and the hydrostatic approximation. Gravity waves are filtered by the implicit integration scheme, permitting a free sea surface elevation. The version of the model used in the standard run and the present experiment has a horizontal resolution of 3.5 x 3.5 degree and 11 vertical layers (centered at depths of 25, 75, 150, 250, 450, 700, 1000, 2000, 3000, 4000 and 5000 m). Topography is included, as well as a one-layer thermodynamic sea-ice model with viscous rheology. The annual cycle is resolved in the model, but in this paper only annual mean values are shown.

For the momentum flux forcing at the upper boundary, the monthly mean wind stress climatology of Hellerman and Rosenstein (1983) was used. The temperature in the surface layer was computed by a Newtonian type coupling to prescribed monthly mean air temperatures derived from the COADS data set (Woodruff et al., 1987), with a coupling coefficient of 40 $Wm^{-2}K^{-1}$ (in the absence of sea-ice). This yields a time constant of approximately 2 months for a surface layer thickness of 50m. In the first spinup-run, the salinity surface boundary condition was a similar Newtonian coupling to the observed

annual mean surface salinity of Levitus (1982). From the steady state solution, an effective freshwater flux was determined. In the following experiments, this freshwater flux was then taken as boundary forcing acting on the surface salinity and on the surface elevation, while still retaining the relaxation to the prescribed atmospheric temperature as the temperature boundary condition. Again, the model was integrated until a steady state was achieved. Details of the initialization can be found in Mikolajewicz and Maier-Reimer (1990).

This type of boundary conditions was first proposed by Stommel (1961) and has been used in several OGCM experiments during the last years. In the absence of a coupled atmospheric model, these "mixed" boundary conditions may be regarded as a reasonably approximate description of the feedback between the ocean and the atmosphere. Anomalies of the sea surface temperature (SST) are damped out by the resultant anomalous atmosphere-ocean heat fluxes, while anomalies in the surface salinities have no influence on the net fresh water flux. Thus, anomalies in the salinity distribution have much longer lifetimes than anomalies of the SST, as indicated by observations.

## 2.2 The White Noise Freshwater Flux Experiment

Short-term atmospheric fluctuations influence the ocean at the upper boundary through surface temperature, wind stresses and freshwater fluxes. In this experiment, the stochastic forcing was restricted to the fresh water fluxes. Because of the lack of feedback mechanisms for the surface salinity, this seems to be the most important contributor on time-scales of decades and longer. The freshwater flux forcing applied was white in time and spatially coherent on the synoptic scale of the atmosphere, to represent the short-term atmospheric variability. The forcing had a globally averaged standard deviation of 16mm/month. Details of the construction of the fresh water flux forcing field can be found in Mikolajewicz and Maier-Reimer (1990).

In the open ocean, the standard deviation of the net freshwater flux is almost constant at a level of 15 mm/month. Towards the coasts, the amplitude generally increases. In the almost closed basins of Hudson Bay and the Mediterranean, the amplitudes have a maximum. This is a consequence of the

design of the stochastic forcing, but may be regarded as an approximate description of the increased variability of the freshwater fluxes in enclosed basins and near the coasts due to the effects of runoff processes. A comparison with data from a 10 year AGCM-simulation (ECHAM3/T42) forced with observed SST (K. Arpe, personal comm.) shows that this amplitude of the forcing is reasonable for high latitudes, although it significantly underestimates the tropical variability. The integration was carried out for 3800 years and the data were stored as means over 2 years. Details of this experiment (hereafter called stochastically forced experiment, STO) as well as its mean climate have been described in Mikolajewicz and Maier-Reimer (1990, 1991).

## 3. Analysis Technique

In the present study, the multivariate Principal Oscillation Pattern (POP) technique was used to investigate the space- and time-dependent variability of surface and sub-surface data in the STO experiment. In contrast to the EOF analysis, which is designed to yield an optimal representation of the covariance structure in the data and not represent dynamical modes in general, the POP analysis is constructed to capture the linear dynamics of the system. The POP analysis provides a simultaneous analysis of both the spatial (e.g. propagating) features and the frequency characteristics of the data. Examples for the good agreement between the theoretical modes of a complex system and those estimated by a POP analysis are given by Schnur et al. (1993).

The main approach of the POP concept, as originally proposed by Hasselmann (1988) and developed and discussed in detail by von Storch et al. (1988), is to model the time evolution of the system by a first order autoregressive vector process

$$\mathbf{x}(t+1) = \mathbb{B}\mathbf{x}(t) + \text{white noise} \qquad (3.1)$$

where $\mathbf{x}$ represents a vector time series (the n dimensional vector formed from $\mathbf{x}(r,t)$ with r=1..n (grid) points). The process matrix $\mathbb{B}$ is given by the lag 1 covariance matrix (von Storch et al., 1988) and can be estimated from the

data. The eigenvectors of $\mathfrak{B}$ are POPs. Generally, $\mathfrak{B}$ is not symmetric and so some or all of its eigenvalues $\lambda$ and corresponding eigenvectors $\mathbf{p}$ occur in complex conjugate pairs. Notice that in this brief outline only complex POPs are discussed. Each state $\mathbf{x}(t)$ may be expressed in terms of the eigenvectors

$$\mathbf{x}(t) = \sum_j z_j(t)\mathbf{p}_j. \tag{3.2}$$

If we disregard the index for convenience, the contribution $\overline{\mathbf{P}}(t)$ of a complex conjugate pair of patterns $\mathbf{p},\mathbf{p}^*$ to the process $\mathbf{x}(t)$ is given by

$$\begin{aligned} \overline{\mathbf{P}}(t) &= z(t)\mathbf{p}+\left[z(t)\mathbf{p}\right]^* \text{ or} \\ \overline{\mathbf{P}}(t) &= z_1(t)\mathbf{p}_1-z_2(t)\mathbf{p}_2, \end{aligned} \tag{3.3}$$

with $2z(t)=z_1(t)+iz_2(t)$. $\mathbf{p}_1$ and $\mathbf{p}_2$ are the real and imaginary part of the eigenvector and $z_1(t)$ and $z_2(t)$ are the coefficient time series of the POP. Their evolution in the absence of noise forcing is described by

$$z_1(t+1) + iz_2(t+1) = \lambda\left[z_1(t) + iz_2(t)\right]. \tag{3.4}$$

If we represent the eigenvalue $\lambda$ by

$$\lambda = |\lambda|\exp(i\omega), \tag{3.5}$$

the oscillation period and e-folding time are given by, respectively

$$T = 2\pi/\omega \tag{3.6}$$

and

$$\gamma = -1/\ln|\lambda|. \tag{3.7}$$

In the absence of white noise forcing, the real and imaginary components of the coefficients vary coherently and 90 degree out of phase, so that the system generates stochastic sequences

$$\circ\circ\circ \longrightarrow \mathbf{p}_2 \longrightarrow \mathbf{p}_1 \longrightarrow -\mathbf{p}_2 \longrightarrow -\mathbf{p}_1 \longrightarrow \mathbf{p}_2 \longrightarrow \circ\circ\circ \qquad (3.8)$$

Thus, if the system at time t=0 is in the state $\mathbf{p}_2$, a quarter of period T later, it will be with high probability in the state $\mathbf{p}_1$, half a period later in the state $-\mathbf{p}_2$, and so on. The correlation over successive phases of the oscillation is determined by the decay time. On average a POP with a decay time of an oscillation period can be observed over a full oscillation cycle, whereas if the decay time is half an oscillation period, typically only half an oscillation cycle can be observed.

The phase $\varphi$ of a POP is arbitrary. For the physical interpretation of the eigenvector, it may sometimes be useful to define this phase factor in a certain way. Note that the kind of definition of $\varphi$ does not change the contribution $\overline{\mathbf{P}}(t)$ to the process $\mathbf{x}(t)$. In the present study, we have defined the phase factor in such a way that the skewness of the imaginary part of the POP coefficient time series was minimized.

Criteria to decide whether a POP contains physically meaningful information are given by von Storch et al. (1988). The most important information is contained in the cross spectrum of the POP coefficients. Both time series should be significantly coherent and 90 degree out of phase in the neighborhood of the oscillation period.

## 4. The Decadal Mode of the North Atlantic

The POP analysis was performed for the upper level salinity fields in the North Atlantic between $95^{o}$ West and $25^{o}$ East and north of $30^{o}$ North. It reveals one dominant mode (Figure 1) on a time-scale of 10 to 40 years. A positive salinity anomaly, developing in the southwest Labrador Sea (imaginary part, Figure 1a), spreads over the entire Labrador Sea and the Northern North Atlantic (Figure 1b, real part; note that the sign of the oscillator is arbitrary). An inspection of the POP coefficient time series, reveals that the behavior of the POP is quite irregular, characterized by time-scales between at least 10 and 40 years. The small ratio (about 0.5) of the decay time (20 years) and oscillation period (40 years) of the eigenvalue implies that only

**Figure 1.**

Salinity anomalies in psu in the second model layer (75 meters) as identified with the POP technique. Note that the isolines are 0.02, 0.05, 0.10 and 0.15psu. Areas with negative values are shaded.

a) Imaginary part of the mode.

b) Real part of the mode.

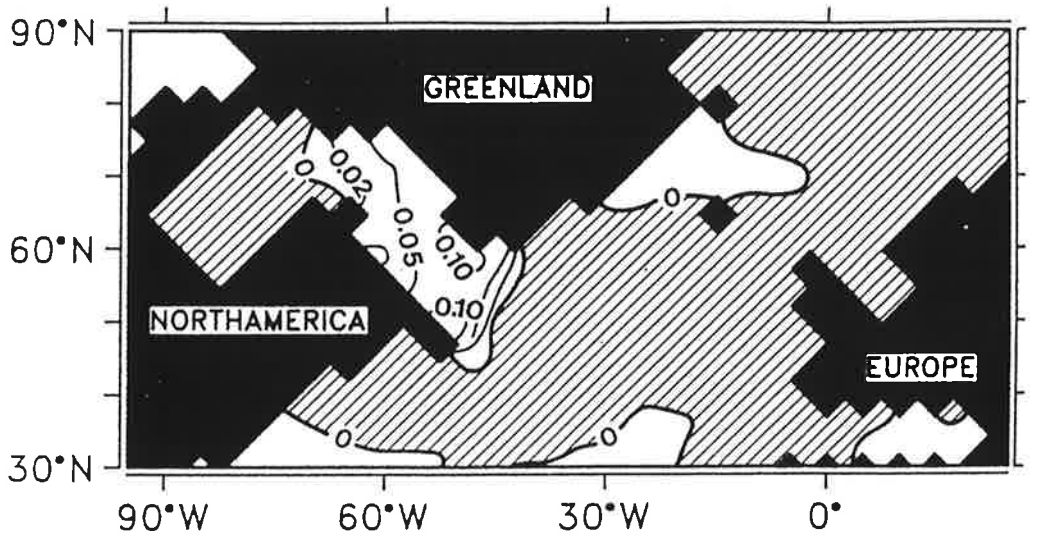


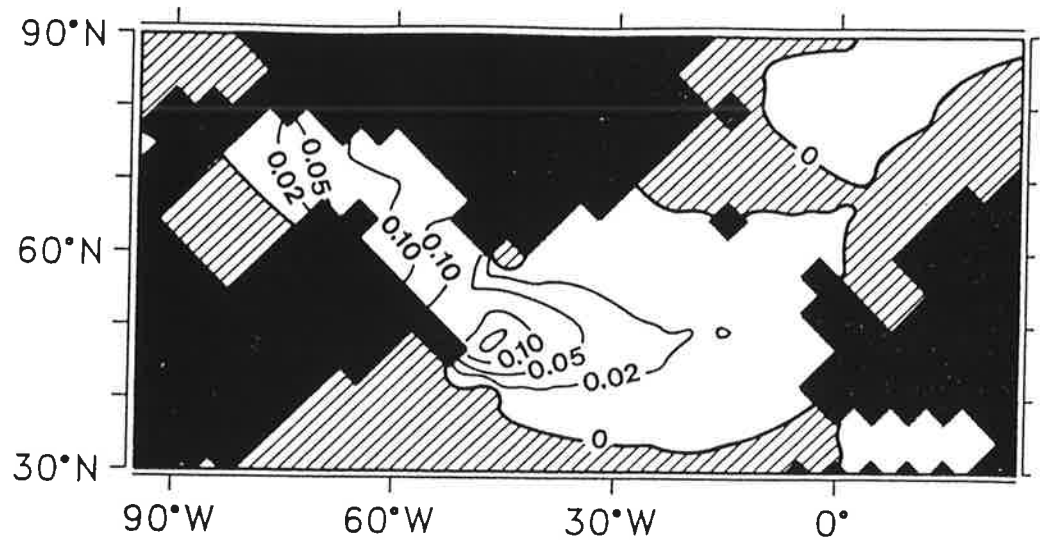

**Figure 2.**
Amount of explained local variance of the decadal mode in the North Atlantic salinity fields (75 meters).

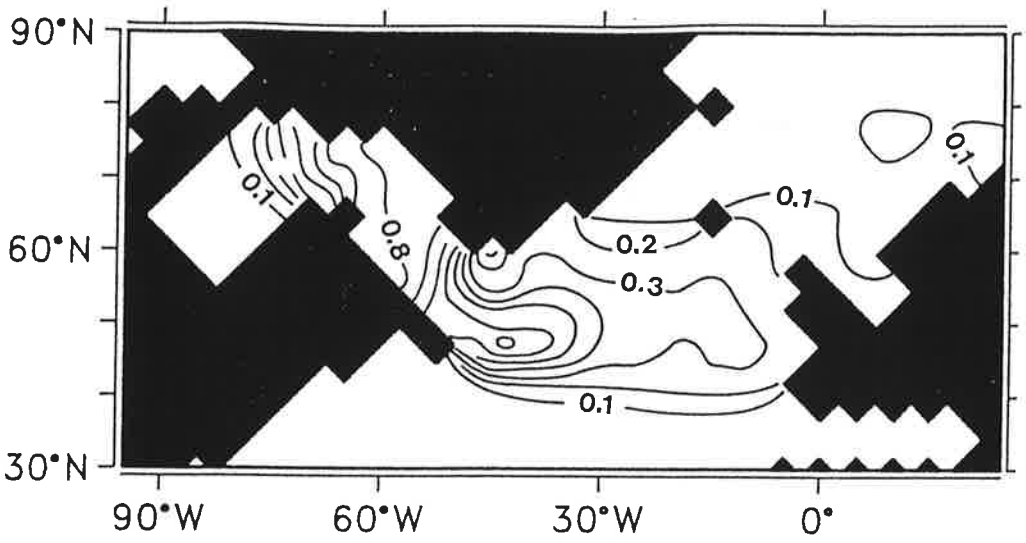

the accumulation of a positive or negative salinity anomaly in the Labrador Sea (imaginary part) and the following propagation (real part) into the North Atlantic can be observed. This decadal mode explains up to 80% of the total variance of the upper level salinity fields in the Labrador Sea and still about 30% in the Northern North Atlantic (Figure 2).

The POP coefficient time series are highly coherent in a range of about 10 to 100 years. They are 90 degree out of phase between about 30 to 40 years, but the phase lag is roughly 60 degrees at 50 years and 120 degrees at 20 years. This corresponds to an almost constant delay of roughly 7 to 8 years between the real and imaginary part of the POP coefficient time series (Figure 3). There are no pronounced peaks in the variance spectra of these time series, as would be expected for an oscillation driven by white noise. Instead, these spectra are rather similar to those of stochastic climate models with simple linear feedback terms.

Furthermore, the response is non-Gaussian. The distribution of the real POP coefficient time series shows a clear asymmetry, whereas the distribution of the imaginary part of the POP coefficient time series is symmetric (Figure 4). Thus, the generation of salinity anomalies in the Labrador Sea, a process that is mainly described by the imaginary part of the POP (Figure 1a), is Gaussian distributed, while the discharge and propagation of the anomalies in the North Atlantic (real part, Figure 1b) is not: the frequency of large positive salinity anomalies in the uppermost levels of the North Atlantic is greater than that of large negative ones.

A possible explanation for these asymmetries is the change in the convection induced by the salinity anomalies: the stratification of the Labrador Sea in the model is strong and quite stable, while the stratification is weak in the North Atlantic between about $50^{o}$ and $60^{o}$ North (Figure 5). A negative salinity anomaly, once developed in the Labrador Sea and advected into the North Atlantic by the mean circulation, stabilizes the water column and suppresses convection. No feedback or amplification of the anomaly occurs. However, a positive anomaly which reaches the weakly stratified region will turn on deep convection, bringing cold and less saline water downwards and warm and more saline water to the surface. This will be observed as an amplification of the positive salinity anomaly at the surface.

**Figure 3.**

Spectra of the POP coefficient time series in the STO experiment.

a) Variance spectra (full line: real component; dashed line: imaginary component). The bar on the right hand side represents the 95% confidence interval.

b) Phase spectrum.

c) Coherence spectrum.

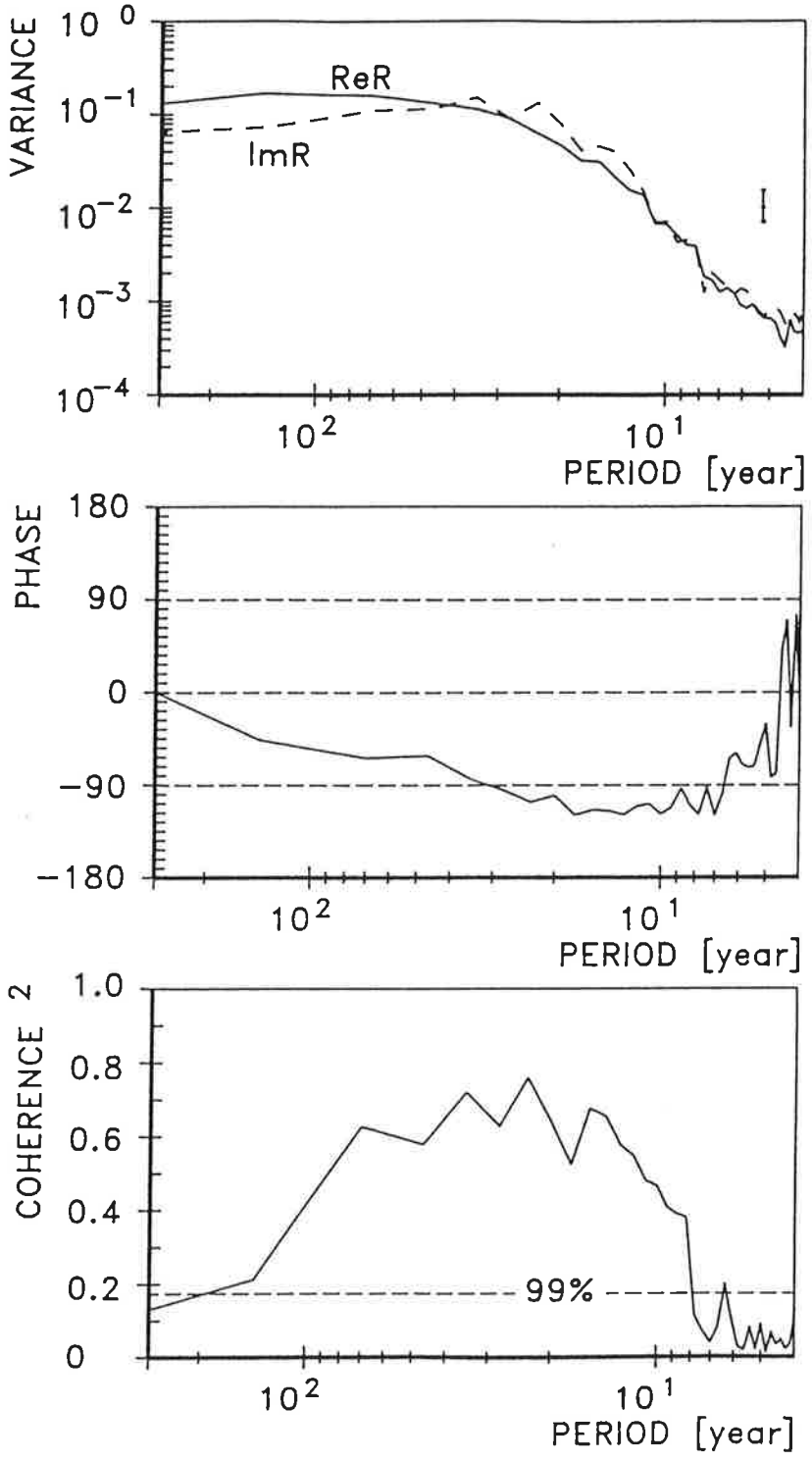

**Figure 4.**

Estimated probability distribution of the amplitudes of the POP coefficient time series.

a) Real part (Skewness is 1.08).

b) Imaginary part (Skewness is $10^{-5}$).

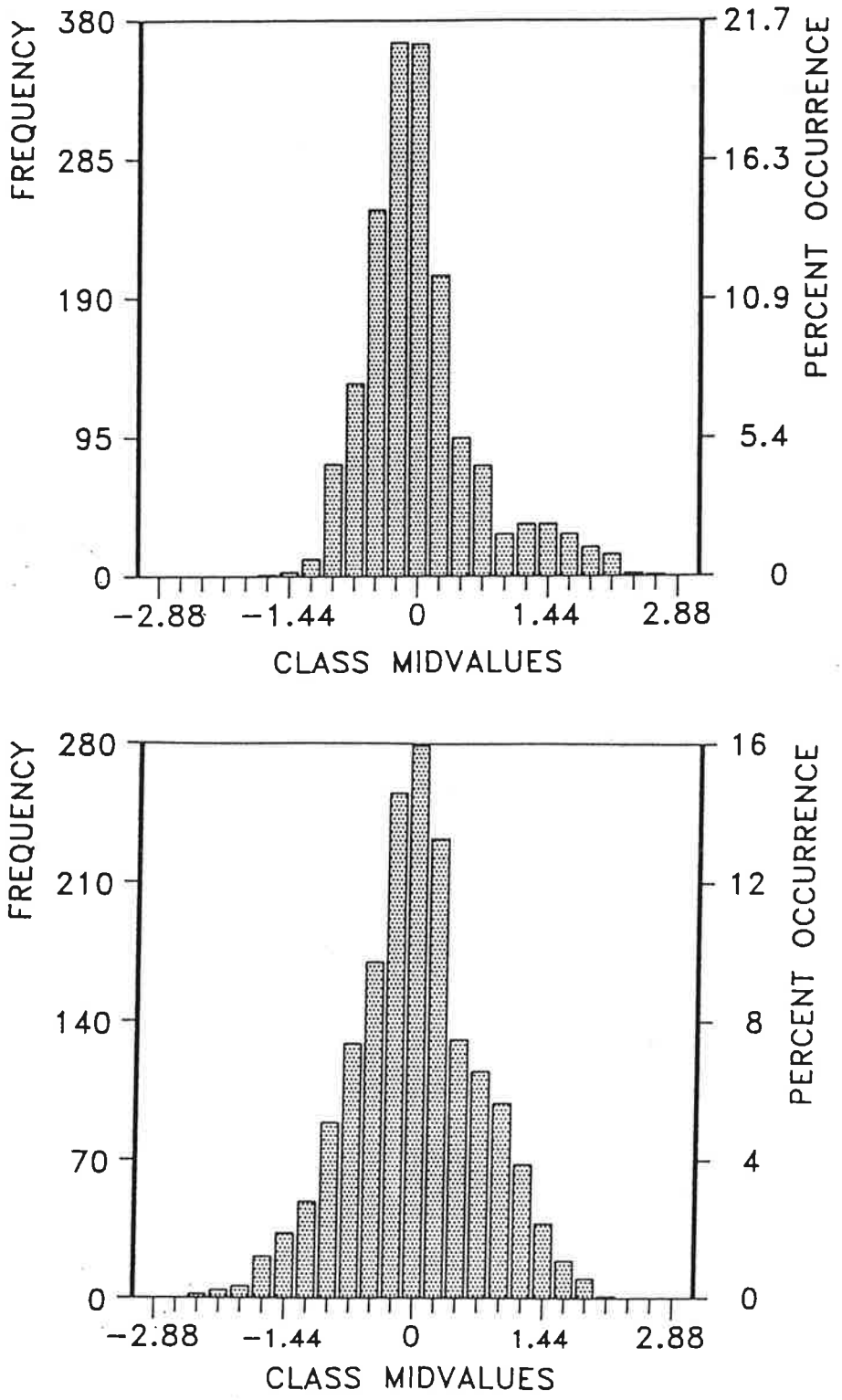

**Figure 5.**

Mean potential density distribution $\sigma_T$ for winter conditions in the Labrador Sea (thick) and the Northern North Atlantic (thin).

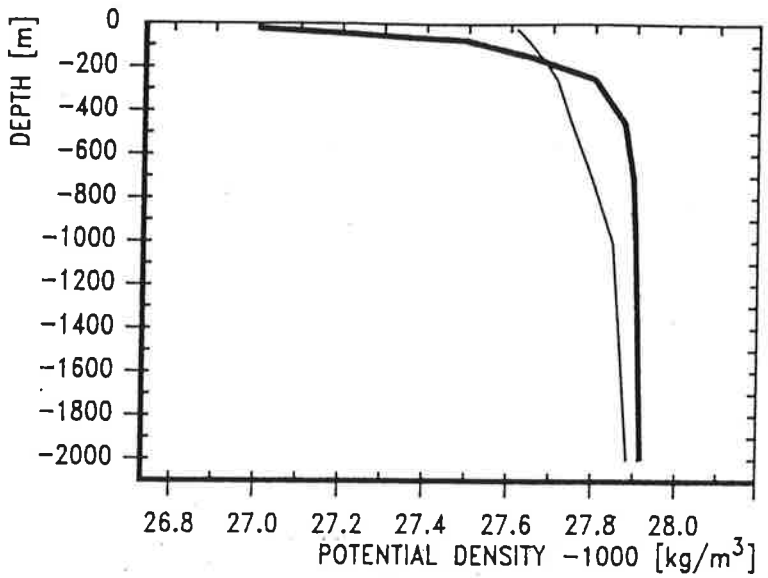

As the variance spectra of the POP coefficient time series, as pointed out, are very similar to those of stochastic climate models with simple linear feedback terms (Figure 3), we hypothesize that in the Labrador Sea (a semi-closed basin in the model which has only limited exchange with the open ocean) an undisturbed straightforward integration of the white noise fresh water flux anomalies takes place. A feedback term is determined by the flushing time $\tau$ of a well mixed upper layer in the Labrador Sea in which the freshwater flux is integrated.

If we neglect the Hudson Bay, a relatively shallow basin in the model, the surface of the Labrador Sea in the model is about $3.2 \times 10^{12} m^2$. The strong stratification indicates that a layer of about 250m is involved in the fresh water integrating process (Figure 5). Thus, the magnitude of the characteristic volume (V) is estimated to be about $8 \times 10^{14}$ $m^3$. The mean net outflow (O) for layers of this depth is about 2.5 Sverdrups. So a rough estimate of the flushing time

$$\tau = \frac{V}{O} \tag{4.1}$$

is approximately 10 years. This time-scale is supported by the decorrelation time, estimated from the upper level salinity fields in the STO experiment (Figure 6). This time is about 10 years on an average in the Labrador Sea and the regions of the North Atlantic, through which the anomalies are advected, in a good agreement with the estimated flushing time.

Using this a priori information about $\tau$ we can calculate the "integrated" fresh water flux **FW** by

$$\mathbf{FW}(t) = \int_0^t \mathbf{fw}(t') \exp\left(-\frac{(t-t')}{\tau}\right) dt', \tag{4.2}$$

where **fw** is the vector time series of the white-noise fresh water flux forcing. This integrated fresh water flux represents the amount of fresh water which, according to our hypothesis, is actually (anomalous) stored in the Labrador Sea. It is thus directly related to the salinity anomalies obtained in the STO experiment and to the thickness of a well mixed upper layer. If our hypothesis is correct, the correlation between the integrated fresh water flux

**Figure 6.**
Decorrelation time in years of the salinity fields in 75 meters in the STO experiment.

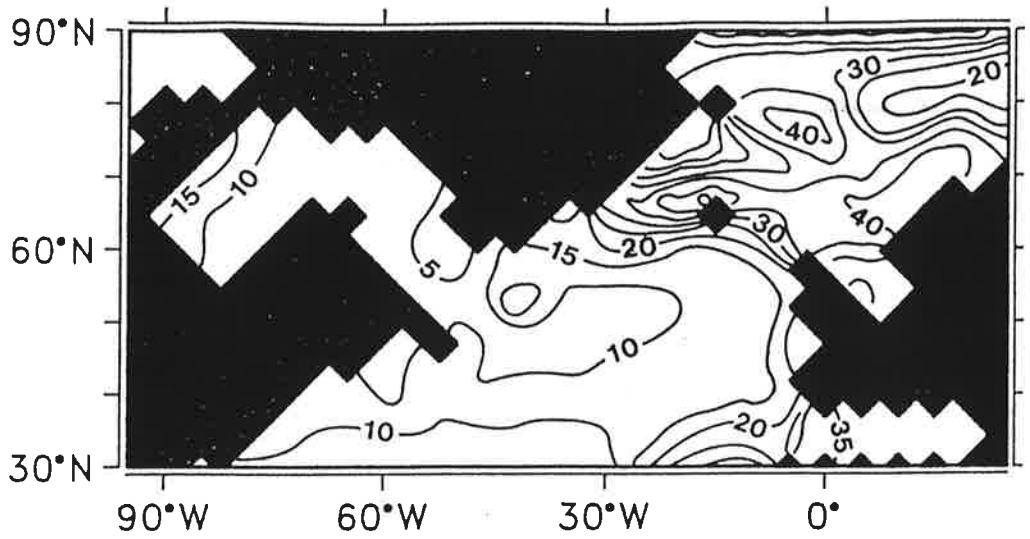


**Figure 7.**
Point to point correlation between the salinity anomalies in the STO experiment and the integrated fresh water fluxes using an estimated time constant of $\tau$=10 years.

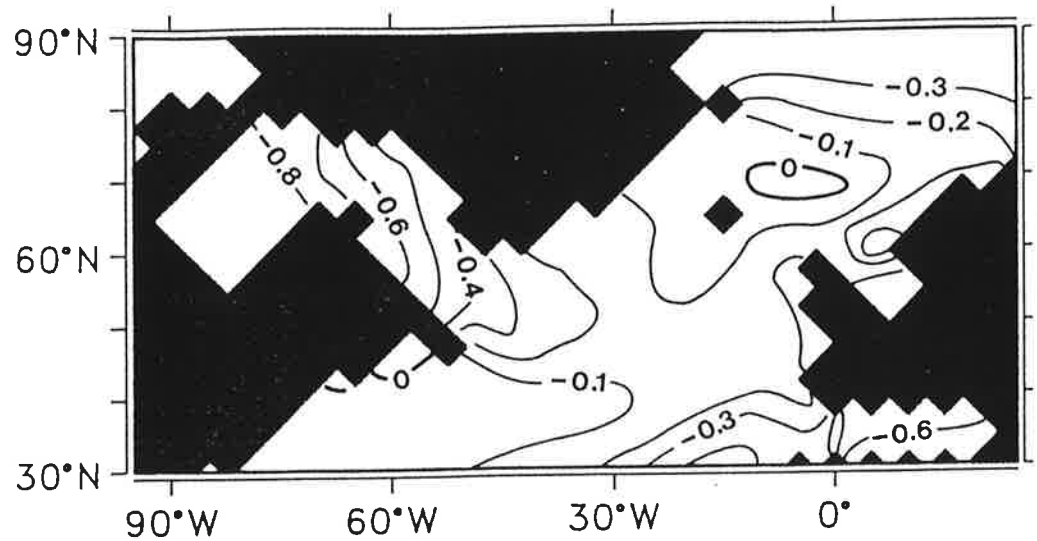

and the upper level salinity anomalies obtained from the STO experiment should be high in all regions where the influence of other processes acting on the salinities (e.g. advection, convection) vanishes or is at least small. We thus expect high correlations in the Labrador Sea and low correlations in the open ocean, where the internal dynamics are more important.

We calculated point to point correlations between the upper level salinity anomalies from the STO experiment and the integrated fresh water fluxes using the simple model (4.2) and a damping time of $\tau$=10 years. In agreement with our hypothesis, we found the highest correlations in relatively closed regions (Figure 7), especially the Labrador Sea (correlations of 0.6 to 0.7). Thus, local fresh water flux integration appears to be the major cause of the salinity anomalies observed in these regions in the stochastically forced experiment.

## 5. Sensitivity Experiments

### 5.1 Stochastic Forcing of the Labrador Sea and the Complementary Experiment

To support this hypothesis, we performed two complementary sensitivity experiments. First we applied the same white noise forcing as in the stochastically forced experiment, but restricted it to the Labrador Sea. In all other parts of the world oceans the climatological fresh water fluxes were used instead. In the other experiment (hereafter complementary experiment) the stochastic forcing was applied everywhere, except in the Labrador Sea, where the fresh water flux was kept to its climatological values. If the POP from the STO experiment could be identified in the first experiment, but not in the complementary experiment, this would further support our hypothesis and the importance of the local fresh water flux forcing in the Labrador Sea. In both experiments the integration was carried out for 500 years.

To compare the results from these experiments with the STO run, we projected the salinity anomaly fields from the sensitivity experiments onto the POP patterns derived from the STO run (Figure 8). In the experiment in which the

**Figure 8.**

a) Salinity anomalies in 75 meters within the first 500 years of the STO experiment averaged over the Labrador Sea. A mean value of 34.15psu was subtracted.

b) POP coefficient time series of the decadal mode in the STO experiment for the first 500 years. The real part is solid, the imaginary part is dashed.

c) Coefficient time series obtained by the projection of the local Labrador Sea stochastic forcing experiment onto the STO mode.

d) Coefficient time series obtained by the projection of the complementary experiment onto the STO mode.

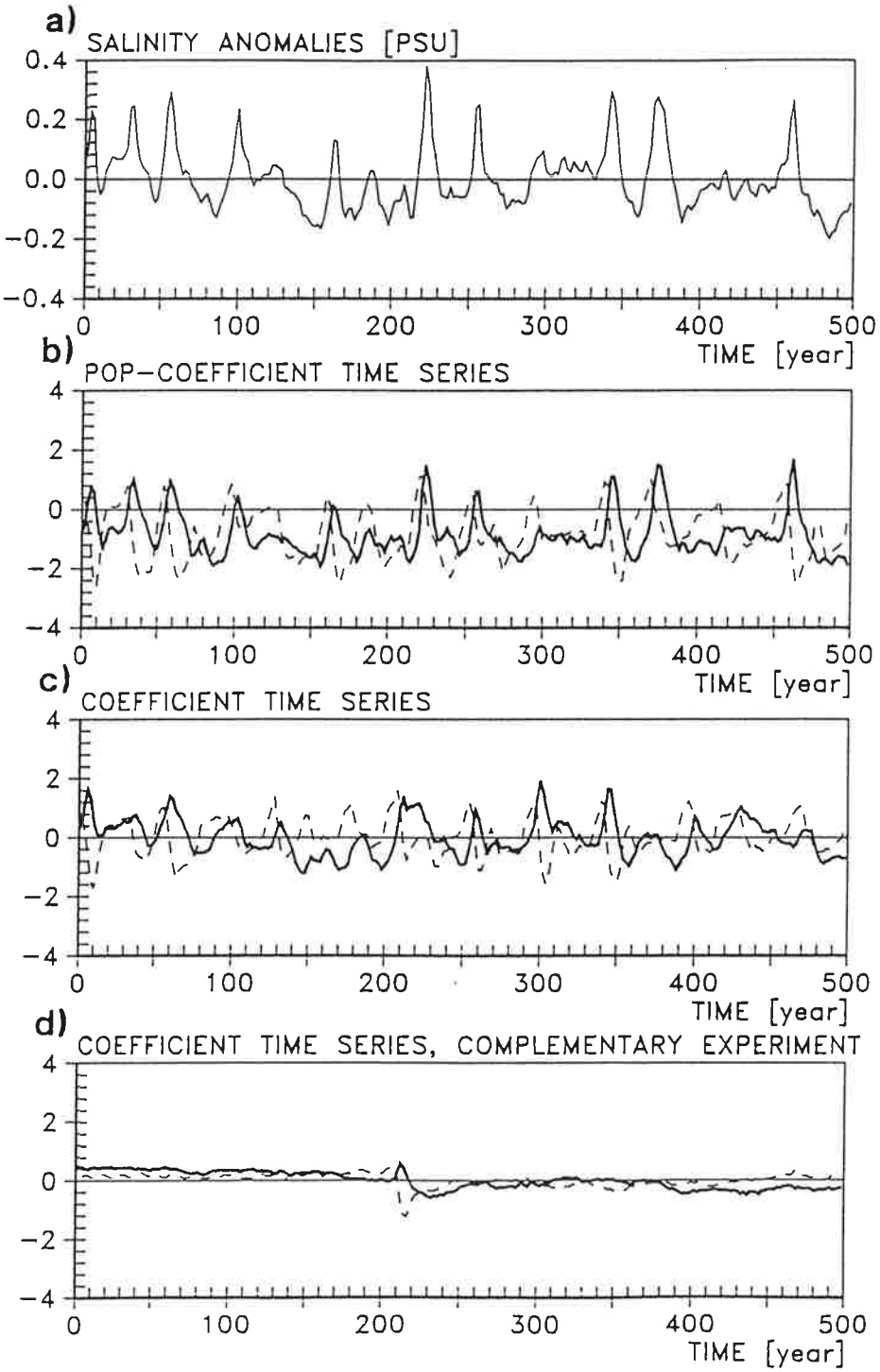

**Figure 9.**

Spectra of the coefficient time series obtained by the projection of the local Labrador Sea stochastic forcing experiment onto the STO mode.

a) Variance spectra. (full line: real component; dashed line: imaginary component). The bar on the right hand side represents the 95% confidence interval.

b) Phase spectrum.

c) Coherence spectrum.

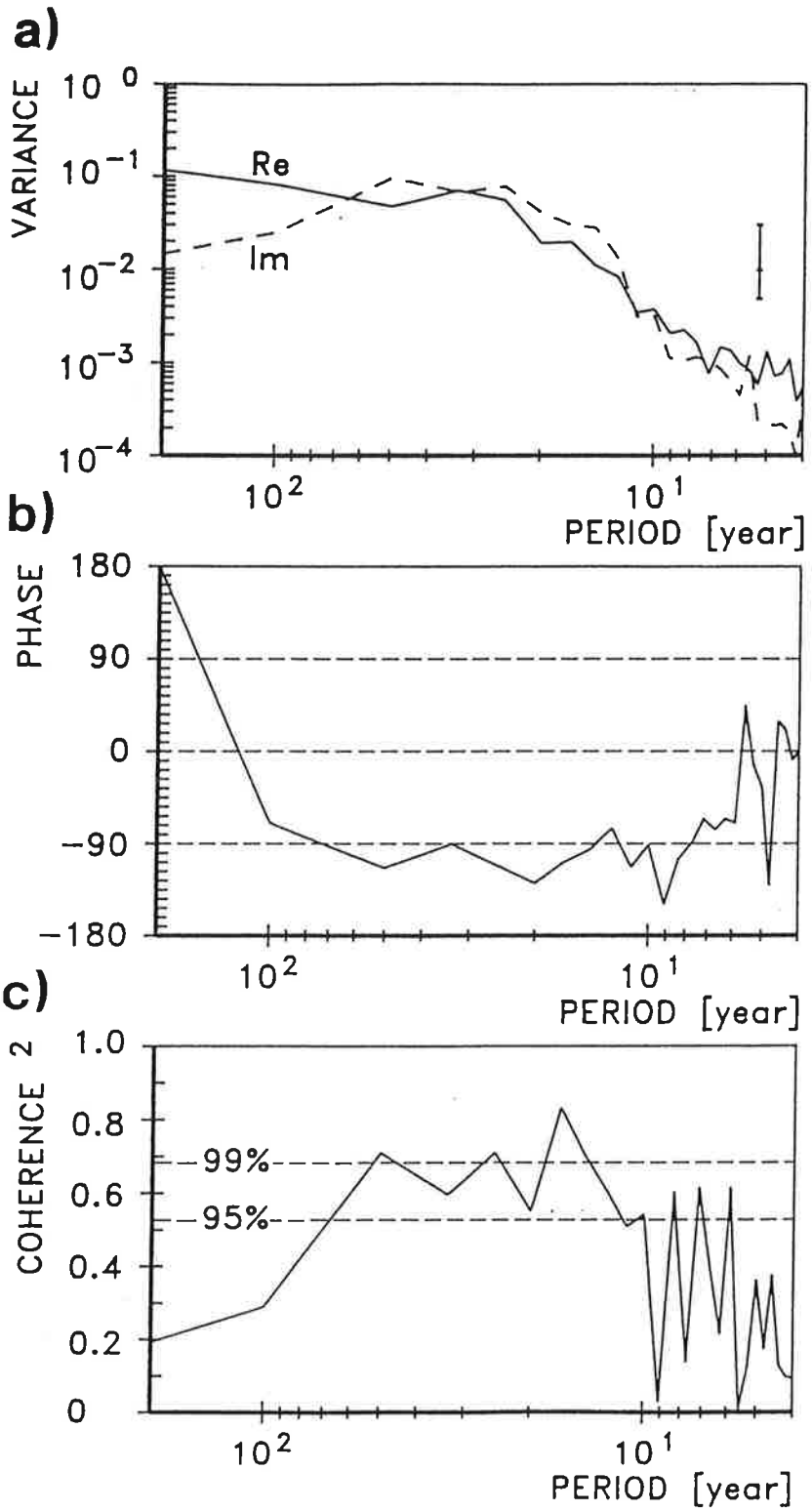

**Figure 10.**

a) Time series of the North Atlantic ocean-atmosphere heat exchange in Gigawatt, derived from the local Labrador Sea stochastic forcing experiment.

b) Thermohaline Circulation Index (THC) describing the maximum of the meridional overturning in the North Atlantic derived from the local Labrador Sea stochastic forcing experiment. An average value of -23.3 Sverdrup is subtracted. Note that the overturning is strongest for negative anomalies. This index is comparable to that of Delworth et al. (1993).

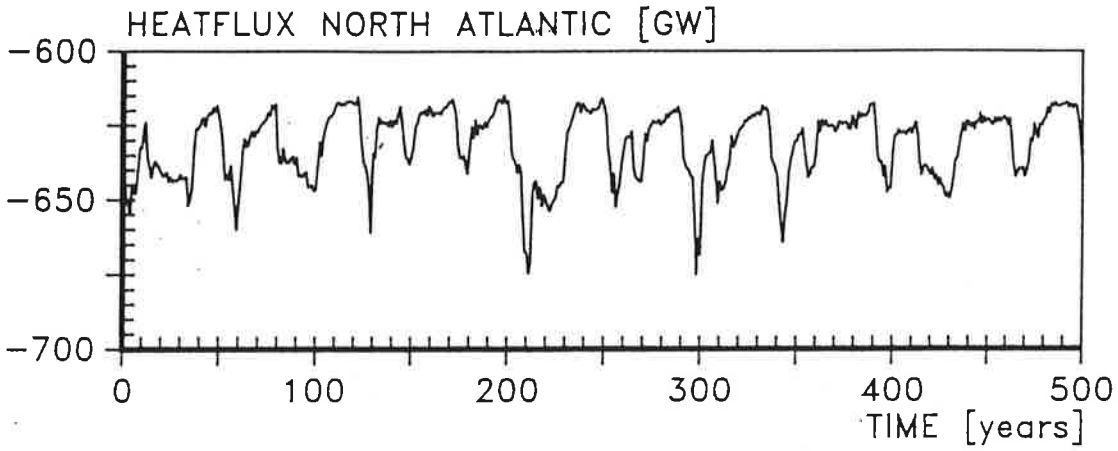


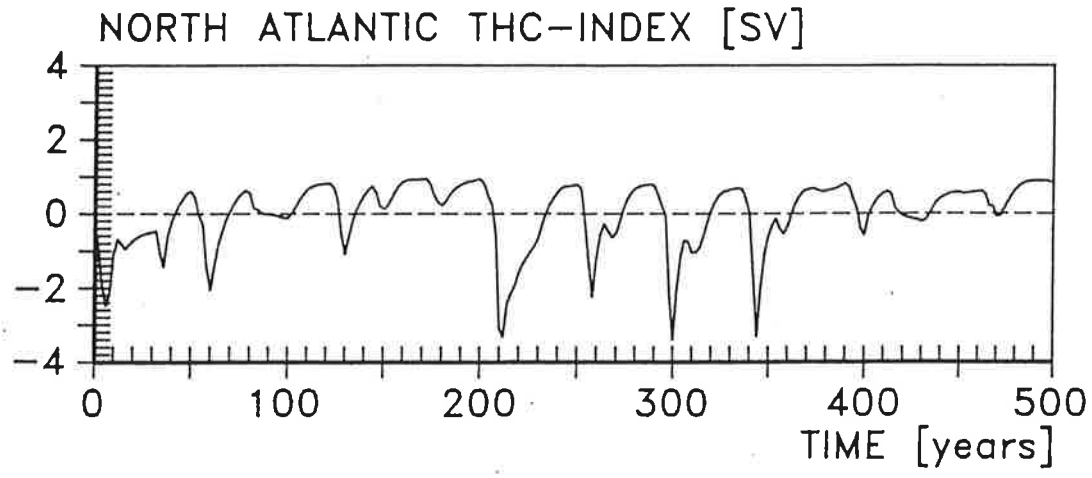

Labrador Sea was stochastically forced, the resulting time series (Figure 8c) are comparable in magnitude and behavior to those of the STO experiment (Figure 8b). Also the spectra of these time series (Figure 9) show a similar variance-, phase- and coherence structure to those of the STO run (Figure 3). In the complementary experiment the mechanism described by the POP was not excited (Figure 8d). Additionally integral quantities like e.g. the atmosphere-ocean heat exchange in the Northern North Atlantic or the meridional overturning show no significant decadal variability in this experiment, but do have considerable variations in the experiment in which the white noise fresh water fluxes were restricted to the Labrador Sea (Figure 10). Both experiments, thus, support the importance of the local fresh water flux forcing in the Labrador Sea for the decadal variability of the Northern North Atlantic.

### 5.2 Directly Forced Salinity Anomalies

To further clarify the identified process and to investigate the differences between the propagation of positive and negative salinity anomalies, we performed a series of sensitivity experiments, in which negative and positive salinity anomalies with several amplitudes were introduced directly into the uppermost layer of the Labrador Sea.

The patterns of the anomalies are similar to the imaginary part of the POP patterns in the STO experiment (Figure 1a). These forcings represent an anomalous integrated fresh water flux or a certain amount of anomalous stored fresh water in the Labrador Sea. The anomalies were induced only at the beginning of the experiments and the integration was carried out over 30 years.

#### 5.2.1 Negative Salinity Anomalies

We projected the anomaly fields onto the POP patterns of the STO run (Figure 11). The resulting time series show a rapid decrease in magnitude, since the initially generated negative salinity anomaly is advected out of the Labrador

Sea. Both time series are lagged, with the imaginary part leading the real part, and thus, describe the advection of the anomalies from the Labrador Sea into the Northern North Atlantic. After about six years, the anomaly has almost vanished. However, anomalies are still found in the Eastern North Atlantic. Since the POP in the STO experiment explains most of the local variances in the Labrador Sea and the Western North Atlantic but is characterized by much smaller amplitudes along the European West Coast, information about the signal from the initially generated salinity anomaly that reaches the European West Coast is lost in the projection on the POP from the STO run. In the Eastern North Atlantic the salinity anomaly is damped out after about 10 to 15 years.

Since there were no changes in this typical behavior, except in the amplitude of the disturbances, we increased the initially generated salt deficit up to $72x10^{12}$ kg. This corresponds to the estimated magnitude of the Great Salinity Anomaly in the Labrador Current (Dickson et al., 1988, his figure 28). Note that this value is based on salinity anomalies at the order of 0.6 to 1.0 psu, whereas the magnitude of a typical event in the STO experiment was only about 0.2 psu.

We estimated the salt deficit that reaches the European West Coast and the Greenland Sea and so finally passes through the Faroe-Shetland Channel by regarding the upper 1000 meters. This was compared with Dickson's et al. (1988) estimates (Figure 12). After six years of integration, a maximum salt deficit of $23x10^{12}$ kg is obtained in the Eastern North Atlantic, compared to Dickson's et al. estimate of about $47x10^{12}$ kg after six years in the Faroe Shetland channel. Beyond this channel, we detected a maximum salt deficit of roughly $6x10^{12}$ kg after about nine years, significantly smaller than Dickson's et al. value of about $16x10^{12}$ kg along the path to the Barents Sea after eight or nine years. Thus, there seem to be some similarities between the GSA and the anomalies in this sensitivity experiment. Especially the time scale (propagation speed) of both anomalies is in good agreement. The anomaly also follows a path similar to that described by Dickson et al. (1988), and the pattern after four years (Figure 13) is similar to that of Levitus (1989b) for the early stages of the GSA. However, our estimates of the maximum salt deficit differ from those of Dickson et al. (1988) by a factor two and more. Dickson et al. (1988) hypothesize that the GSA was advected around the

subpolar gyre, probably reinforced during its long propagation along the Labrador Coast by local freshening. However, in both Dickson's hypothesis and our experiments most of the variability is described by the advection of the anomalies.

### 5.2.2 Positive Salinity Anomalies

In contrast to the negative anomalies the behavior of positive salinity anomalies is not uniform. If the magnitude of an initially generated positive salinity anomaly is smaller than roughly two standard deviations of the STO POP, the behavior is similar to that described for negative anomalies. However, if the amplitude is increased, the behavior becomes quite different (Figure 11). Again, the anomaly spreads over the Labrador Sea and the Northern North Atlantic, yielding patterns similar to the POP patterns. But after approximately four to six years, a strong negative salinity anomaly has developed in the Labrador Sea. The positive anomaly has been advected into the North Atlantic (Figure 11, thin solid line) and decays after approximately 10 to 12 years. Due to the evolution of a negative salinity anomaly in the Labrador Sea, it takes mores time to damp all (positive and negative) disturbances out.

Contrary to the experiments with introduced negative salinity anomalies, in which changes in the mean velocity field were small, the deep ocean and the mean circulation are strongly influenced by the initiated positive salinity anomalies. Through the onset of deep convection in the Labrador Sea, the density in lower layers is increased and the net outflow in the well mixed upper layers is reduced by roughly 30% for the first 4 years after the initialization of the positive salinity anomaly. At the same time the formed deep water spreads out at lower depth. The reduced net outflow in the upper layers reduces the damping of the salinity anomalies and, thus, increases the flushing time (4.1). Since precipitation exceeds evaporation in the Labrador Sea region, the prolongation of the residence time of a water particle at the surface leads to the evolution of a negative surface salinity anomaly after a few years.

**Figure 11.**
Projection of the initially generated negative salinity anomaly (thick) and the initially generated positive salinity anomaly (thin) onto the STO POP; real parts: full lines; imaginary parts: dashed lines.

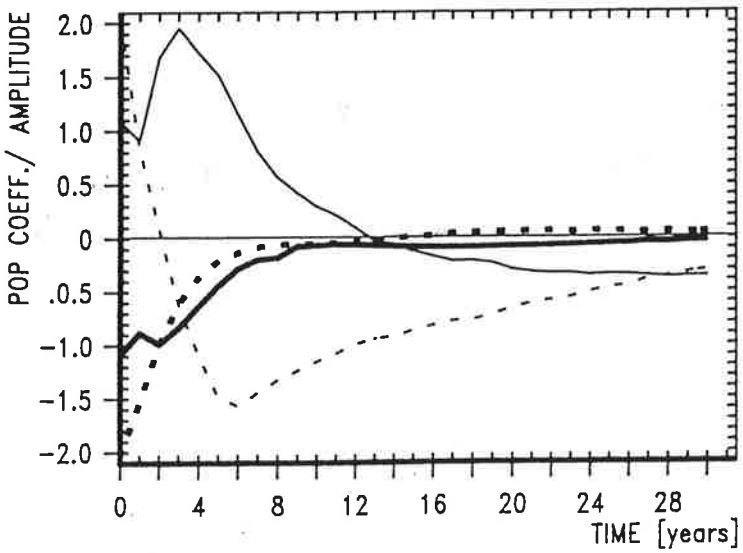


**Figure 12.**
Salt deficit estimated by Dickson et al. (1988) for different years for the Great Salinity Anomaly in the North Atlantic (upper values) and derived from the experiment with an initial negative salinity anomaly (lower values) in $10^{12}$kg.

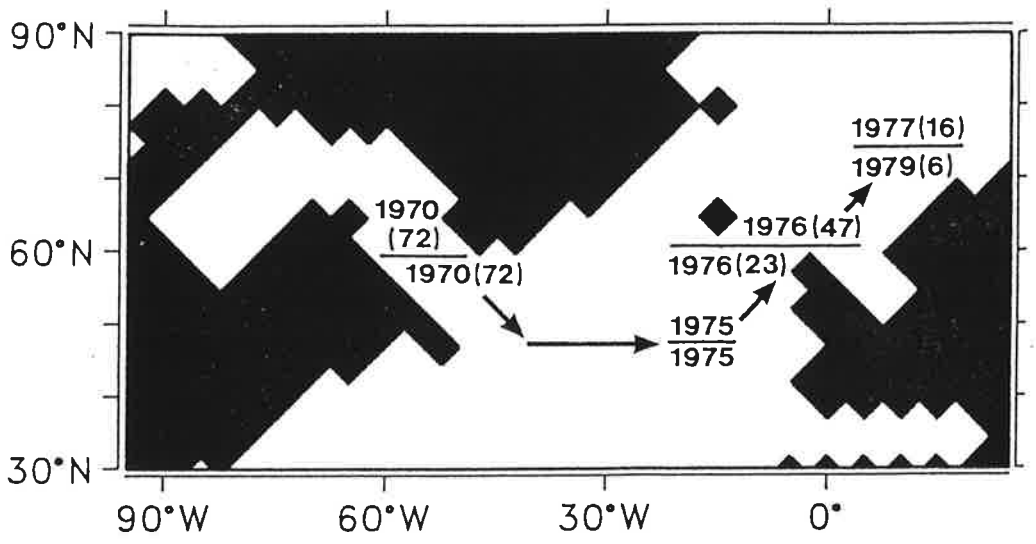

**Figure 13.**
Development of the initial negative salinity anomaly in 75 meters after 4 years.

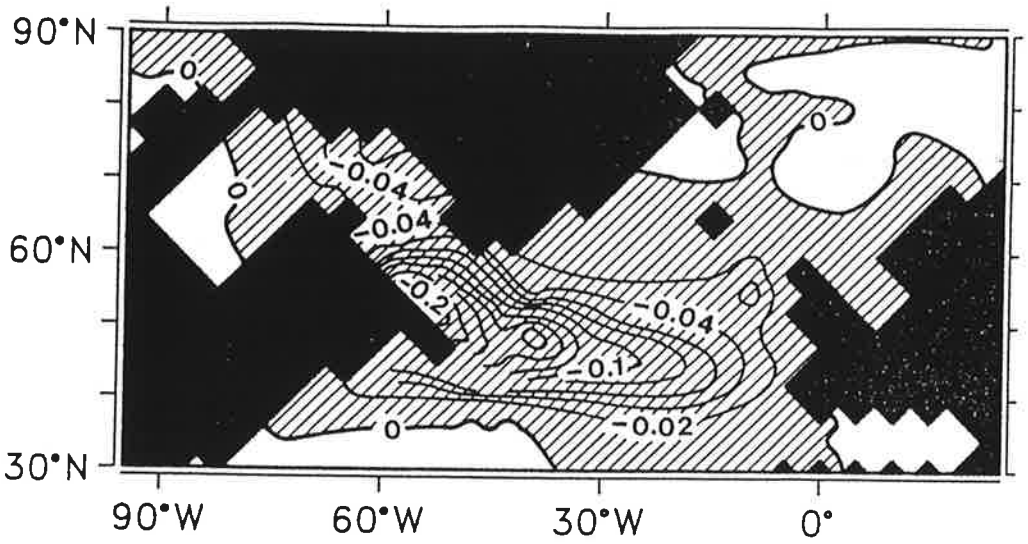

**Figure 14.**

Composites of the salinities in 700m in the experiment in which the stochastic forcing was restricted to the Labrador Sea. The composites were constructed for the five highest (a) and the five lowest (b) values of the coefficient time series obtained by the projection on the POP of the STO experiment.

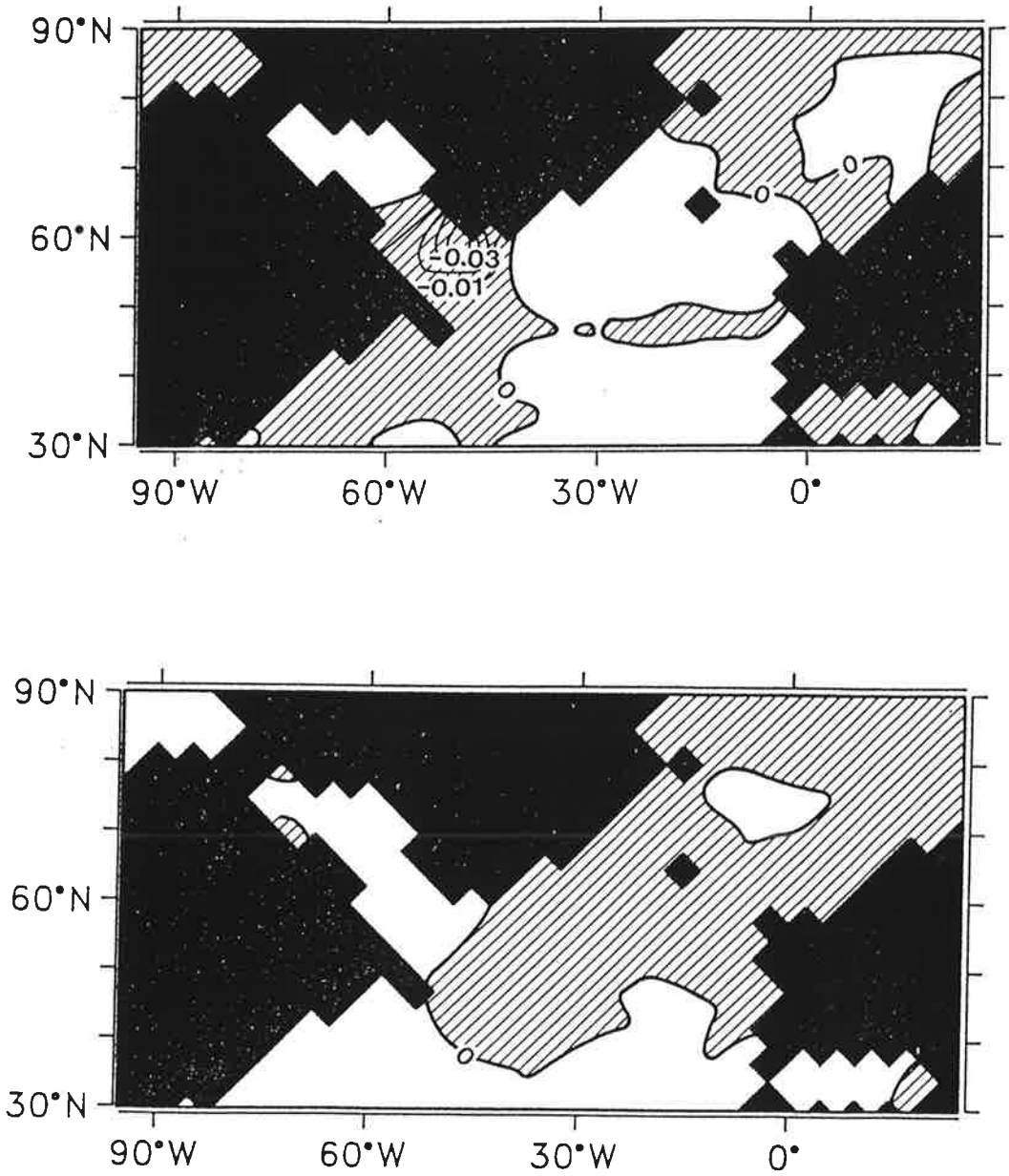

The different impact of positive and negative surface salinity anomalies on the deep ocean can be further emphasized by two composites derived from the experiment in which the stochastic forcing was restricted to the Labrador Sea. We constructed the composites of the salinities in 700m depth for the five highest and lowest values of the real part of the coefficient time series and subtracted the climatological mean (Figure 14). Large positive salinity anomalies in the upper layers strongly influence deep convection and, thus, the deep ocean (Figure 14a). Compared with the lower layers the intensified convection brings more cold and fresh water downward, generating negative salinity anomalies there. In the case of large negative surface salinity anomalies however, the impact at 700m is much weaker (Figure 14b), as indicated by the probability distribution of the POP-coefficient time series (Figure 4) and the results of the sensitivity experiments with directly forced surface salinity anomalies

## 6. Summary and Discussion

Most of the variability in the upper level salinity fields of the Labrador Sea and the Northern North Atlantic in the stochastically forced OGCM experiment could be explained by a decadal mode as identified by the POP technique. This mode describes the accumulation of salinity anomalies in the Labrador Sea and the subsequent advection into the Northern North Atlantic. It is characterized by time-scales of roughly 10 to 40 years. We found that the irregularly occurring salinity anomalies in the Labrador Sea are mainly caused by a straightforward local integration of the white noise fresh water fluxes, since this region is characterized by limited exchange with the open ocean. The time-scale and damping term of the integration process are determined by the flushing time of the well mixed upper layer.

By the restriction of the white noise fresh water flux forcing to the Labrador Sea, we were able to reproduce both the generation and propagation of the salinity anomalies. If the white noise freshwater fluxes were applied everywhere except in the Labrador Sea, no significant decadal variability in the North Atlantic was excited. These experiments emphasize that the source of the variability lies in the Labrador Sea and demonstrate the importance of the

local fresh water flux forcing.

When we forced the model with positive and negative initial anomaly patterns similar to the imaginary part of the decadal POP in the STO experiment, we basically recovered the propagating features of the POP mode. However, the evolution and propagation of once generated strong positive or negative anomalies showed noticeable differences. Negative salinity anomalies show a tendency to spread over the North Atlantic and decay after about 10 to 15 years, whereas sufficiently strong positive salinity anomalies are advected into the North Atlantic and are replaced by a negative anomaly after about 4 to 6 years. This can be explained by the different impacts of the anomalies on the velocity field and the flushing time. The decadal mode, thus, represents a "discharge process", depending nonlinearly on the modulated circulation structure, rather than a regular linear oscillator.

The occurrence of the described phenomenon is hard to identify in the real ocean. A comparison with direct observations is limited by the sparsity of the data base and the coarse resolution of the model. However, a few indications that underlines the importance of the Labrador Sea and the local fresh water flux forcing there, do exist. Several authors (e.g. Clarke and Gascard, 1983, Telley and McCartney, 1982, Read and Gould, 1992) report that the characteristics of Labrador Sea Water (one of the main water masses of the North Atlantic; believed to be formed in the central Labrador Sea by convection) near the source show considerable variations within tens of years. The cause of the variability is attributed to a combination in the rate of renewal and of changes in the properties of the water from which Labrador Sea Water is formed. Variations in the source characteristic can be traced across the North Atlantic, with a circulation time of 18 to 19 years (Read and Gould, 1992). Lazier (1980) showed that the convectively mixed upper layer in the Labrador Sea during the GSA was limited to unusually shallow depth. At the same time an increase in the salinities at the 400 to 1200m levels could be observed. This structure can be identified within typical events in the STO and sensitivity experiments. Negative salinity anomalies lead to a decrease in convection, thus increasing the salinity in levels below 250 to 450m. Strong enough positive salinity anomalies (in the order of 0.2 psu) however, lead to an increase of convection, bringing relatively cold and fresh water (compared with deeper layers) downward, such that negative salinity anomalies are

generated there (Figure 14).

An intercomparison with data show that the travel times of the negative salinity anomalies in our model are in good agreement with the estimates of Dickson et al. (1988) for the Great Salinity Anomaly, and that the pattern after four years (Figure 13) is similar to that of Levitus (1989b) for the early stages of the GSA. This pattern is also similar to the real part of the POP.

Delworth et al. (1993) reported on a self-sustained interdecadal oscillation in the meridional overturning of the North Atlantic in a fully coupled ocean-atmosphere GCM. They ended up with a composite for the surface salinities between years with large and small convective overturning (his Figure 4) that is similar to the real part of the POP in our stochastically forced experiment (Figure 1b). The changes in the meridional overturning associated with these patterns are of similar magnitude (Figure 10b). Delworth et al. (1993) argued that the time scale of their oscillation is determined by horizontal circulation of the North Atlantic. However, in our model the existence of decadal scale variability in the North Atlantic crucially depends on the relative isolation of the Labrador Sea in order for that basin to act as an integrator of the white noise time series of the fresh water flux. No significant decadal variability in the North Atlantic could be excited, if the fresh water flux in the Labrador Sea was kept constant.

We conclude that the basic mechanisms of the decadal mode are the generation of salinity anomalies in the Labrador Sea (in our experiment by variations of the local fresh water flux forcing) and the subsequent advective propagation across the North Atlantic. Significant variations of the atmosphere-ocean heat exchange in the Northern North Atlantic can be produced by variations in the fresh water flux in the Labrador Sea alone. Thus the local integration of highly variable fresh water fluxes in relatively undisturbed areas may produce non-local fluctuations on larger spatial scales that contribute significantly to natural climatic variability on decadal time scales.

## ACKNOWLEDGEMENTS

We thank H. von Storch for valuable discussions on the application of the POP concept, K. Hasselmann, N. Weber, U. Luksch, E. Zorita and S. Kharin for valuable comments on the manuscript, M. Grunert and D. Lewandowski for finishing the drafts, and P. Besemann for the English review. This work was sponsored by the Bundesministerium für Forschung und Technologie via the BMFT project 132 and the Deutsche Forschungsgemeinschaft (DFG) via the Sonderforschungsbereich (SFB) 318.

## REFERENCES:

Bjerknes, J. (1964). *Atlantic air-sea interaction.* Advances in Geophysics, ed., Academic Press, 1-82.

Clarke, R.A. and Gascard, J.C. (1983). *The Formation of Labrador Sea Water. Part I: Large-Scale Processes.* J. Phys. Oceanogr. 13, 1764-1178.

Crowley, T.J. and G.R. North (1991). *Paleoclimatology.* Oxford University Press, New York, 335p.

Delworth, T., Manabe, S. and R.J. Stouffer (1993). *Interdecadal Variability of the Thermohaline Circulation in a Coupled Ocean-Atmosphere Model.* Submitted to J. Climate.

Deser, C. and M.L. Blackmon (1993). *Surface Climate Variations over the North Atlantic Ocean During Winter: 1900-1989.* Submitted to J. Climate.

Dickson, R.R., J. Meincke, S.-A. Malmberg and A.J. Lee (1988). *The "Great Salinity Anomaly" in the Northern North Atlantic 1968-1982.* Prog. Oceanogr. 20, 103-151.

Folland, C.K., T.R. Karl and K.Y. Vinnikow (1990). *Observed Climate Variations and Change.* In J.T. Houghton, G.J. Jenkins and J.J. Ephraims (eds.) Climate Change. Cambridge University Press, Cambridge, 198-238.

Frankignoul, C. and K. Hasselmann (1977). *Stochastic climate models, part II: Application to sea-surface temperature anomalies and thermocline variability.* Tellus 29, 289-305.

Frankignoul, C. and Reynolds, R.W. (1983). *Testing a Dynamical Model for Mid-Latitude Sea Surface Temperature Anomalies.* J. Phys. Oceanogr. 13, 1131-1145.

Hasselmann, K. (1976). *Stochastic climate models, Part I, Theory.* Tellus 28, 6, 473-485.

Hasselmann, K. (1982). *An ocean model for climate variability studies.* Prog. Oceanogr. 11, 69-92.

Hasselmann, K. (1988). *PIPs and POPs: The reduction of Complex Dynamical Systems Using Principal Interaction and Oscillation Patterns.* J. Geophys. Res. 93, D9, 11015-11021.

Hellermann, S. and M. Rosenstein (1983). *Normal monthly wind stress data over the world ocean with error estimates.* J. Phys. Oceanogr. 13, 1093-1104.

Herterich, K. and K. Hasselmann (1987). *Extraction of Mixed Layer Advection Velocities, Diffusion coefficients, Feedback Factors and atmospheric forcing Parameters from the Statistical Analysis of North Pacific SST Anomaly Fields.* J. Phys. Oceanogr. 17, 2145-2156.

Kushnir, Y. (1993). *Interdecadal Variations in North Atlantic Sea Surface Temperature and Associated Atmospheric Conditions.* Submitted to J. Climate.

Lazier, J.R.N. (1980). *Oceanographic Conditions at Ocean Weather Ship Bravo, 1960-1974.* Atmosphere-Ocean 18(3), 227-238.

Lemke, P. (1977). *Stochastic climate models, part 3, application to zonally averaged energy models.* Tellus 29, 385-392.

Levitus, S. (1982). *Climatological Atlas of the World Ocean.* NOAA Professional Paper 13, Rockville Md.

Levitus, S. (1989a). *Interpentadal Variability of Temperature and Salinity at Intermediate Depth of the North Atlantic Ocean, 1970-1974 Versus 1955-1959.* J. Geophys. Res. 94, C5, 6091-61131.

Levitus, S. (1989b). *Interpentadal Variability of Salinity in the Upper 150 m of the North Atlantic Ocean, 1970-1974 Versus 1955-1959.* J. Geophys. Res. 94, C7, 9679-9685.

Maier-Reimer, E. and K. Hasselmann (1987). *Transport and storage of $CO_2$ in the ocean - an inorganic ocean-circulation carbon cycle model.* Climate Dyn. 2, 63-90.

Maier-Reimer, E., U. Mikolajewicz and K. Hasselmann (1993). *Mean circulation of the Hamburg LSG OGCM and its sensitivity to the thermohaline surface forcing*. J. Phys. Oceanogr 23(4), 731-757.

Marotzke, J. (1990). *Instabilities and Multiple Equilibria of the Thermohaline Circulation*. Berichte aus dem Institut für Meereskunde Nr. 194, Kiel, 126 p.

Mikolajewicz, U. and E. Maier-Reimer (1990). *Internal secular variability in an OGCM*. Climate Dyn. 4, 145-156.

Mikolajewicz, U. and E. Maier-Reimer (1991). *One Example of a Natural Mode of the Ocean Circulation in a Stochastically Forced Ocean General Circulation Model*. Strategies for Future Climate Research, ed. M. Latif, Hamburg, 287-318.

Mysak, L.A., T.F. Stocker and F. Huang (1993). *Century-scale variability in a randomly forced, two-dimensional thermohaline ocean circulation model*. Climate Dyn. 8, 103-116.

Rasmusson, E.M. and T.H. Carpenter (1982). *Variations in tropical sea surface temperature and surface wind fields associated with the Southern Oscillation/El Niño*. Mon. Weather Rev. 110, 354-384.

Read J.F. and W.J. Gould (1992). *Cooling and freshening of the subpolar North Atlantic Ocean since the 1960s*. Nature 360, 55-57.

Schnur, R., G. Schmitz, N. Grieger and H. von Storch (1993). *Normal Modes of the Atmosphere as estimated by Principal Oscillation Patterns and derived from Quasi-Geostrophic Theory*. J. Atmos. Sci. 50(15), 2386-2400.

Stommel, H. (1961). *Thermohaline convection with two stable regimes of flow*. Tellus 13, 224-230.

Telley, L.D. and M.S. McCartney (1982). *Distribution and Circulation of Labrador Sea Water*. J. Phys. Oceanogr. 12, 1189-1204.

von Storch, H., T. Bruns, I. Fischer-Bruns and K. Hasselmann (1988). *Principal Oscillation Pattern analysis of the 30-60 day oscillation in a GCM equatorial troposphere.* J. Geophys. Res. 93, 11015-11022.

Weaver, A.J., E.S. Sarachik and J. Marotzke (1991). *Freshwater flux forcing of decadal and interdecadal oceanic variability.* Nature 353, 836-838.

Wigley, T.M.L. and S.C.B. Raper (1990). *Natural variability of the climate system and detection of the greenhouse effect.* Nature 344, 324-327.

Winton M. and E.S. Sarachik (1993). *Thermohaline Oscillations Induced by Strong Steady Salinity Forcing of Ocean General Circulation Models.* Submitted to J. Phys. Oceanogr.

Woodruff, S.D., R.J. Slutz, R.L. Jenne and P.M. Steurer (1987). *A comprehensive ocean-atmosphere data set.* Bull. Am. Meteorol. Soc. 68, 1239-1250.